Journal of Electromagnetic Analysis and Applications, 2024, 16, 43-67
https://www.scirp.org/journal/jemaa
ISSN Online: 1942-0749
ISSN Print: 1942-0730

The Pairing Analysis Improvement of Magnetized Structure in Electromagnetic Bulging Process in Case of Tube with Field Shaper

Blaise Kevine Lenz Soronga[1,2,3], Zhanqian Zhan[1,2,3,4], Jing Liu[4], Jonas Asamoah[5], Mohamed Bangali Bangura[6], Matala Makiese[7], N'kodia Kambani Chrionie[8], Md Jobayer Hossain[9], Yongdong Chen[10]

[1]Program Debugging and Design Department, Guangdong Lyric Robot Automation Co., Ltd, Huizhou, China
[2]Electrical and Automation Department, China Three Gorges University, Yichang, China
[3]Electronic Department, Power Electronic Research Center, University of Kent, Giles Ln, Canterbury, UK
[4]Program Debugging Department, Guangdong Lyric Robot Automation Co., Ltd., Huizhou, China
[5]Electrical and Computer Engineering Department, South China University of Technology, Guangzhou, China
[6]World Standardization, Certification and Testing Group (Shenzhen) Co., Ltd., Shenzhen, China
[7]Electrical Engineering-Power System, Mapon University, Kindu, Democratic Republic of Congo
[8]Department of Economy Managment, School of Management, Computer and Telecomunication, Rabbat, Marocco
[9]Materials Visual Calibration Department, Guangdong Lyric Robot Automation Co., Ltd., Huizhou, China
[10]Program Design Department, Guangdong Lyric Robot Automation Co., Ltd., Huizhou, China

Email: Lenzkevin95@gmail.com, zhanzhanqian@dingtalk.com, king2392@dingtalk.com, jsarbinbeasamoah@gmail.com, joelmatala50@gmail.com, Mohamedbangali01@gmail.com, Chrionienkodia@gmail.com, 1554944205@qq.com

How to cite this paper: Soronga, B.K.L., Zhan, Z.Q., Liu, J., Asamoah, J., Bangura, M.B., Makiese, M., Chrionie, N.K., Hossain, MdJ. and Chen, Y.D. (2024) The Pairing Analysis Improvement of Magnetized Structure in Electromagnetic Bulging Process in Case of Tube with Field Shaper. *Journal of Electromagnetic Analysis and Applications*, **16**, 43-67.
https://doi.org/10.4236/jemaa.2024.164004

Received: March 7, 2024
Accepted: April 27, 2024
Published: April 30, 2024

Abstract

In the current practical science, the accuracy in the formability of metal alloys being the goal when using electromagnetic forming (EMF) technology, which is a high-speed processing technology that uses Lorentz forces to achieve plastic deformation of sheet metal; according to the previous analysis, the results have shown that in most cases, the Lorentz force acting on the workpiece (metal) is not uniform, there are uneven axial deformations of the metal plates which prevent the rapid advancement of today's technology. In this article, we presented some advanced analyzes which will lead us to improve the technical solution for the problems of non-uniform axial deformations of the metals in the traditional tube electromagnetic forming technology (EMF). A field shaper is used as a practical forming tool to influence the magnetic field and magnetic pressure distribution, thereby improving the forming ability and result during the electromagnetic forming (EMF) process and we see that induced eddy current control is realized by changing the structural parameters of the magnetic field shaper; which improves the strength and controllability of the magnetic force that acts on the workpiece; thereby a greater radial magnetic pressure can be achieved with field shaper than the case without it; the field shaper regulates the electromagnetic force, the distribution of the magnetic pressure decreases, and the uniform force area of the tube increases which effectively enhances the uniform range of the pipe electromagnetic bulging and the electromagnetic induction coupling between the coil and the metallic workpiece is generally required to produce the Lorentz forces. Using COMSOL Multiphysics® simulation software helped us to accurately represent the real world, simulating multiple physical effects that happened in this model during the process.

Keywords

Electromagnetic Forming, Field Shaper, Lorentz Force, Magnetic Pressure Distribution

1. Introduction

Electromagnetic forming (EMF) is a technology that employs electromagnetic-force pulsation to realize metallic workpiece processing [1] [2]. Compared with conventional mechanical based processing, EMF can improve plastic deformation ability of materials and enhance their forming limit about 5 to 10 times due to its high strain rate (10^3 - 10^5 s^{-1}) [3] [4]. Because the electromagnetic force is of a non-contact nature [5] [6]. EMF is able to improve the surface quality of the formed workpiece [7] [8]. The magnetic pulsed forming is a high-speed forming method, which uses the electromagnetic body force to drive an electrically conductive workpiece into deformation [9] [10]. It can be considered as one of the best high-rate forming methods from the several aspects such as high cleanness, cost-efficiency (reduced number of operations and lower energy cost), no lubricant is required, productivity and electromagnetic forming eliminates the risk of explosion forming, it is more convenient than electro-hydraulic forming [11] [12]. Automotive, aerospace, nuclear, machinery, electronics light chemical industry, weapon industry and medical sectors may like to use this process (EMF) due to the specific requirement and performance; when applying this technique, it is also possible to improve the formability of some materials such as aluminum (Al) that is a good candidate material for use in automotive industrial and many other applications [13] [14]. This makes it possible to avoid undesirable forming of conventional quasi-static methods like wrinkling, tearing, uncontrolled spring back and any unexpected effects on the metal workpiece.

2. Literature Review

From the end of 1950s, electromagnetic forming developed rapidly and became a new technology of metal plastic processing, which was highly valued by industrial countries. Depending on the workpiece, the electromagnetic forming technology can be divided into three classes; electromagnetic sheet forming, electromagnetic tube reducing or compression and electromagnetic tube expanding or tube expansion, respectively [15].

Each of these types and several methods of forming have been considered. Figure 1 and Figure 2 show respectively the General scheme of electromagnetic forming & typical forming configurations and three different processes of electromagnetic forming.

Actually, cylindrical driving coil is usually used in tube electromagnetic bulging.

However, due to the end effect of this structure of forming coil the radial electromagnetic force exerting on the middle section of the tube is much larger than the ones at both ends which results in poor tube uniformity in the axial direction; two solutions were proposed:

1) A tube electromagnetic bulging method using a concave driving coil had been proposed to realize uniform tube radial deformation by weakening the electro-magnetic force in the middle of the tube.

2) Tube electromagnetic bulging method based on convex coil that can not only improve the uniformity of tube radial deformation, but can also restrain the issue of tube wall thickness thinning during the EMF process was presented.

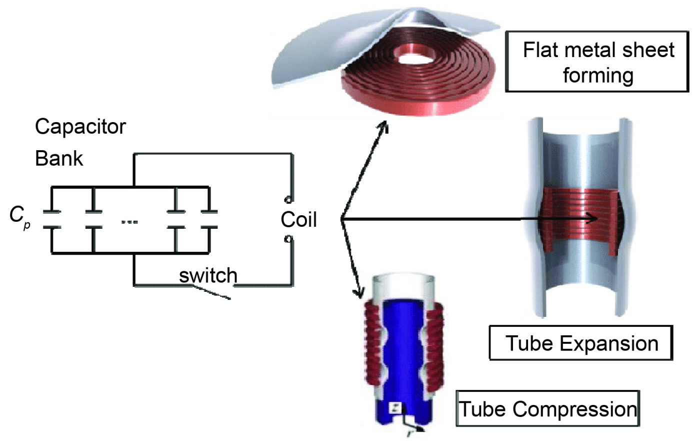

Figure 1. General scheme of electromagnetic forming & typical forming configurations.

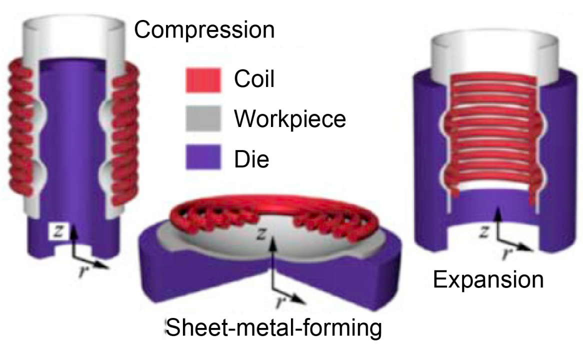

Figure 2. Three different processes of electromagnetic forming.

Neither of these two was giving the engineers the desired results.

A solution was found that in addition to the direct EMF of workpiece using a driving coil, a **field shaper** can be used to adapt the electromagnetic force profile [16] [17]. As a main part of EMF system, a Field shaper concentrates the magnetic field in desired points of the metal workpiece during the forming process [18]. A field-shaper transmits the energy produced by inductor system to the expected points. It is clear that any where we transmit the energy, there is some energy dissipation in transmitter cause to decrease the efficiency of the system, therefore applying a field-shaper decreases the efficiency of an EMF system. The same EMF setup can be applied for several types of forming and there is no need to replace the coil system in order to modify the magnetic field for a special case.

3. The Principle of EMF and Magnetic Field Shaper

In the early stages of the electromagnetic bulge system, it mainly consisted of charging system, discharge capacitor, switch, drive coil, tube fitting (the part) and a direct current circuit [19]. The charging system of traditional tube EMF system first charges the capacitor, then closes the switch and the energy stored in the capacitor is transferred to the drive coil in the form of pulse current. In this system, the capacitor acts as a pulse feed through a discharge switch to the main drive coil and formed tube [13] [20]. The large impulse current generated in the coil results in an induced eddy current in the tube which is placed close to the coil according to the law of electromagnetic induction [21]. The magnetic field generated by the coil itself superimposes on the induced eddy current generated on the tube fitting to produce the electromagnetic force that causes the tube to bulge (accelerate the tube and deformation). The main structure of an EMF system:

- Capacitor bank for storing the electrical energy (The required energy to be discharged).
- Fast closing switch (for breaking and connecting the circuit).
- Work coil (for creating magnetic field in the Work zone).
- Workpiece/tube/metal (Which is to be contracted or expanded or shaped).
- Form-defining Die or matrix (which gives to the tube the desired shape).
- Field shaper, which controls the magnetic field distribution.

The constitutive elements of the basic EMF system are shown in **Figure 3** and **Figure 3** shows the main traditional EMF system.

In the process of the EMF, the coil is often subjected to huge electromagnetic force, which affects the lifespan of the coil moreover, in the traditional coil tube electromagnetic bulging system, because the height of the driving coil is usually less than or equal to the height of the tube, the axial magnetic flux density is much larger than the radial magnetic flux density, so that the tube is subjected to a larger radial electromagnetic force, resulting in a large reduction of wall thickness [22]. And the radial electromagnetic force is not uniformly distributed in the axial direction, which leads to the bulging of the tube into an axially uneven convex shape.

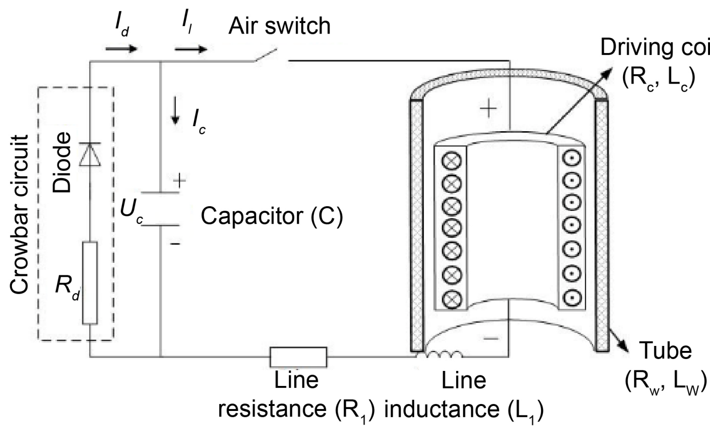

Figure 3. Traditional EMF system.

Figure 4 shows the Eddy current distribution within the tube (EMF expansion).

Based on the Maxwell's equations, the method in **Figure 2** can be expressed as:

$$\nabla \times \boldsymbol{E}_\Phi = -\frac{\partial \boldsymbol{B}_z}{\partial t} + \nabla \times \left(\boldsymbol{V}_z \times \boldsymbol{B}_r\right) \tag{1}$$

$$\boldsymbol{J}_\Phi = \gamma \boldsymbol{E}_\Phi \tag{2}$$

where $\boldsymbol{E}$ is the electric field intensity, $\boldsymbol{B}_r$ is the radial magnetic flux density, $\boldsymbol{B}_z$ is the axial magnetic flux density, $\boldsymbol{V}_z$ is the plate axial velocity, GAMMA is the plate conductivity, and $\boldsymbol{J}$ is the ring induced eddy current density [23]. The electromagnetic force exerting on the tube is mainly composed of axial component, $\boldsymbol{F}_z$ that can be calculated from:

$$\boldsymbol{F}_z = \boldsymbol{J} \times \boldsymbol{B}_r \tag{3}$$

From the above equation, the electromagnetic force distribution plays an important role in controlling the quality of the metal sheets forming process. As it can be seen from (3) the electromagnetic force distribution is determined by the induced eddy current and the magnetic flux density.

4. Circuit parameters of the EMF system

4.1. Circuit of the Traditional Sheet Electromagnetic Forming

The electromagnetic analysis in the tube bulging process is based on the equivalent circuit and the following one is the equivalent circuit without magnetic Field shaper.

Figure 5 shows the equivalent circuit of EMF process without Magnetic Field shaper.

Due to the high temperature generated during the EMF process; a discharge circuit with a resistor is used to dissipate the temperature rise of the coil through the resistor [24] [25]. The discharge circuit can be modeled as a second-order RLC zero input circuit.

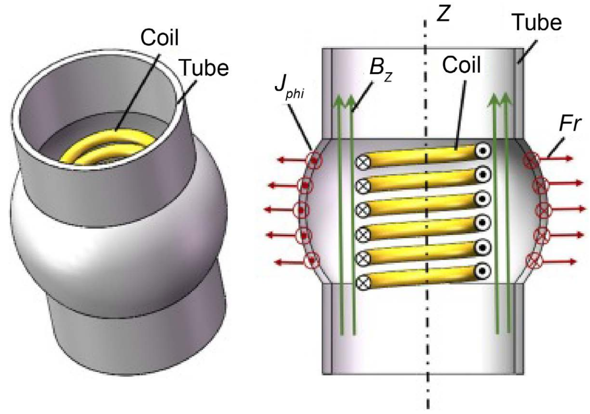

Figure 4. Eddy current distribution within the tube (EMF expansion).

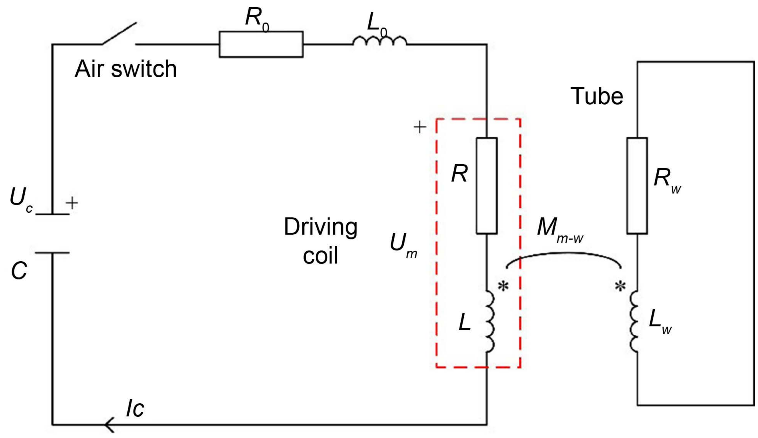

Figure 5. Equivalent circuit of EMF process without Magnetic Field shaper.

According to the Kirchhoff's law:

$$\begin{cases} \boldsymbol{U}_c = \boldsymbol{U}_c + \boldsymbol{U}_{coil} \\ \boldsymbol{U}_c = R_o \boldsymbol{I}_c + L_o \dfrac{\mathrm{d}\boldsymbol{I}_c}{\mathrm{d}t} \\ \boldsymbol{U}_{coil} = R\boldsymbol{I}_c + L\dfrac{\mathrm{d}\boldsymbol{I}_c}{\mathrm{d}t} + M_{m\text{-}w}\dfrac{\mathrm{d}\boldsymbol{I}_w}{\mathrm{d}t} \\ \boldsymbol{U}_c = \boldsymbol{U}_o - \dfrac{1}{C}\displaystyle\int_0^t \boldsymbol{I}_c \mathrm{d}t \end{cases} \tag{4}$$

$$\begin{cases} \boldsymbol{I}_{coil} + \boldsymbol{I}_c - \boldsymbol{I}_d = 0 \\ \boldsymbol{R}_w \boldsymbol{I}_w + \boldsymbol{L}_w \dfrac{\mathrm{d}\boldsymbol{I}_w}{\mathrm{d}t} + M_{m-w}\dfrac{\mathrm{d}\boldsymbol{I}_c}{\mathrm{d}t} = 0 \end{cases} \tag{5}$$

$$\begin{cases} \boldsymbol{I}_d = 0, \boldsymbol{U}_c \ge 0 \\ \boldsymbol{I}_d = \dfrac{\boldsymbol{U}_c}{\boldsymbol{R}_d}, \boldsymbol{U}_c < 0 \end{cases} \tag{6}$$

4.2. EMF with Field Shaper Equivalent Circuit

The ignorance of the direct coupling between the workpiece and the coil take place when a magnetic field shaper is added to discharge circuit [24].

Figure 6 shows the Equivalent circuit of EMF process with Magnetic Field.

For this circuit is modified thus according to the Kirchhoff's law,

$$\begin{cases} \boldsymbol{I}_{coil} + \boldsymbol{I}_c - \boldsymbol{I}_d = 0 \\ R_f \boldsymbol{I}_f + L_f \dfrac{\mathrm{d}\boldsymbol{I}_f}{\mathrm{d}t} + M_{f\text{-}m} \dfrac{\mathrm{d}\boldsymbol{I}_c}{\mathrm{d}t} + M_{f\text{-}w} \dfrac{\mathrm{d}\boldsymbol{I}_w}{\mathrm{d}t} = 0 \\ R_w \boldsymbol{I}_w + L_w \dfrac{\mathrm{d}\boldsymbol{I}_w}{\mathrm{d}t} + M_{w\text{-}f} \dfrac{\mathrm{d}\boldsymbol{I}_f}{\mathrm{d}t} = 0 \end{cases} \tag{7}$$

From this set of equations (4), (5), (6), (7), we have:

$\boldsymbol{C}_o$ is the capacitance,

$\boldsymbol{U}_c$ is the capacitor voltage,

$\boldsymbol{U}_o$ is the capacitor voltage at the initial state (Discharge voltage),

$\boldsymbol{U}_l$ is the line voltage of the discharge circuit,

$\boldsymbol{R}_o$ is the line resistance,

$\boldsymbol{R}_d$ is the crowbar resistance,

$\boldsymbol{L}_o$ Line inductance,

$\boldsymbol{I}_d$ is the current in the freewheeling circuit,

$\boldsymbol{I}_{coil}$ is the driving coil current,

$\boldsymbol{I}_w$ is the induced eddy current in the workpiece.

5. Methodology

5.1. Research Analysis

Currently, due of the advantages and good development prospects of electromagnetic forming in the field of metal forming, following the research method of this article, we have pointed out some research analysis about what is happening in this process. However, as an industrial processing technology, the EMF technology of sheet metal parts to be processed is far from mature, and there is still room from improvement.

The followings are the critical research analysis during this process:

(1) The service lifespan of the coil. The electromagnetic force of electromagnetic forming comes from the change of the electromagnetic field caused by the

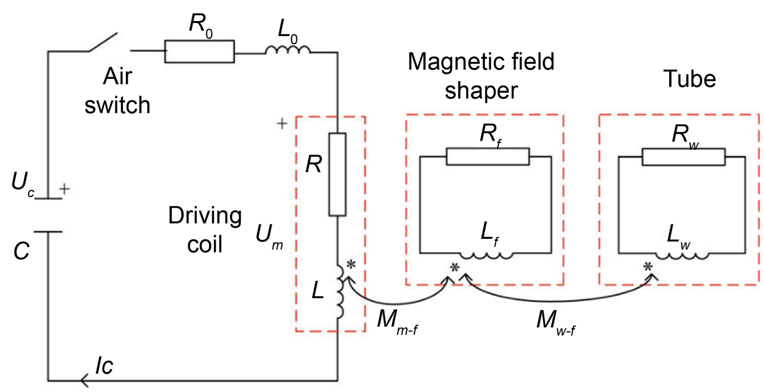

Figure 6. Equivalent circuit of EMF process with Magnetic Field shaper.

instantaneous appearance of the strong pulse current, which produces the electromagnetic force of the shaping. This causes the coil to be subjected to high-intensity electromagnetic fields, high-intensity voltage and current, high-intensity stress, and a large amount of Joule heat during the operation, so that the service lifespan of the coil in most cases is very short, which tremendously increases the cost of electromagnetic forming. Although it is possible to delay the aging process of the coil by means of electromagnetic gradual forming, these methods are not mature enough, which cause them to have fatal defects at present, therefore it cannot be considered as a long-term solution.

At present, the lifespan problems of coils are mainly categorized into two categories, that is, the problems of structural strength and Joule heat. In response to the problem of structural strength, foreign scholar Grovaschenko found that the damage of the coil mainly starts from the place with a small radius of curvature, and it can be considered to increase the strength of the coil by strengthening the facilities.

(2) The electromagnetic force used in electromagnetic forming can only generate electromagnetic force perpendicular to the metal plate to be processed because the spatial structure of the electromagnetic field that generates the electromagnetic force is relatively simple. This leads to the fact that in actual processing, the deformation of the workpiece to be processed is mainly bulging, the deformation method is single, the resulting part structure is relatively simple, and the application area is narrow, which cannot meet the current demand for rapid progress in complex structure processing.

(3) The current electromagnetic forming technology can only be used to machine smaller parts, but not large parts, because of the limitations of the equipment that generates the electromagnetic force. If the electromagnetic forming technology is used to process large parts, the coils and field shaper of the electromagnetic forming equipment will be too large, which will keep on increasing the cost.

Initially in the EM Forming process, the energy is stored in the pulsed power generator as capacitive energy, and this energy is further utilized to deform the workpiece.

Figure 7 shows the methodology energy transfer diagram during the electromagnetic forming.

A complex energy transfer is observed in between these two stages (initial tube shape and deformed tube). Only a certain amount of the stored energy is transferred to the coil and used to deform the workpiece. We will notice that there are losses in between energy storage and the deformation of workpiece during the deformation procedure. The capacitor charging energy $\boldsymbol{E}_c$ at first is transferred into a magnetic pressure pulse $\boldsymbol{p}$; this magnetic pressure pulse is transferred into kinetic energy $\boldsymbol{E}_{kin}$ and then transferred into forming energy $\boldsymbol{E}_{def}$. During deformation process there is a moment when the pressure exerted on the tube has decreased to zero, the kinetic energy stored in the workpiece is used to finish the

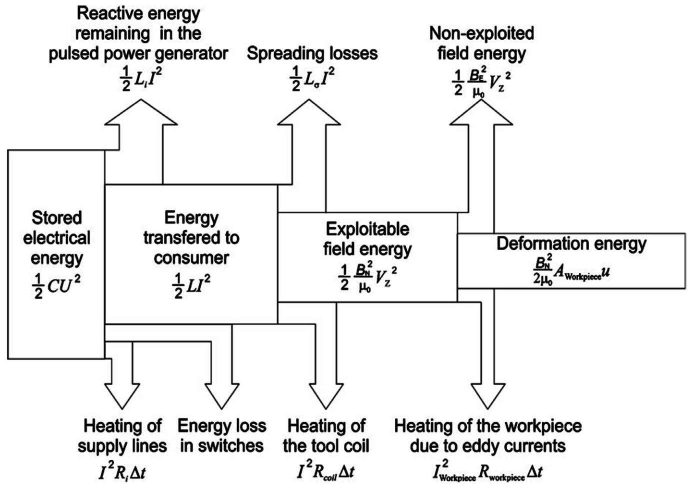

Figure 7. Methodology Energy transfer diagram during electromagnetic forming.

forming process.

In this Article, the materials of forming coil are limited to metals having low resistivity to minimize the loss caused by adiabatic heating during the forming process. Also, we consider that the materials should have sufficient mechanical strength and mass to keep stability and withstand the repulsive force during the forming process. Beryllium copper, Aluminum (Al) alloy and Copper (Cu) are usually used due to their high mechanical and electrical properties such as yield strength and low electric resistance as shown in Table 1.

The workpiece shows different dynamic behaviors depending on the shapes of the forming coils. Thus, the forming coils should be designed considering the shapes of the products to be produced.

5.2. Tube Material and Data Collection

EMF process is capable of deforming electrically conductive metals only, it is found that in most cases Aluminum and its alloys, copper and its alloys, Magnesium and its alloys and many more are the most used material when performing the EMF process. In this work we have selected the Aluminum alloys Al 6061and Al 5083 for our improvement. AA 6061 is aluminum alloy that has generally good mechanical properties and is treatable and weldable; it is mainly composed of magnesium and silicon alloying elements. The chemical composition of a AA6061 tube is shown in the following tables.

5.2.1. AA 6061

AA 6061 has a strong performance because of its mechanical charachteristic which is involving its mechanical properties. We can find its chemical composition in Table 2 and Table 3.

5.2.2. AA 5083

The detailed geometrical structure of the proposed model is described below:

Table 1. Coils mechanical and electrical properties for forming.

Material	Hardness (Vickers)	Electrical Resistivity (ohm-m)	Permeability (u)
Al 6061	75	4.32e−8	1
Cu 12200	50	1.70e−8	1
Becu17000	90	2.94e−8	1

Table 2. The chemical composition of a AA6061.

Constituent	Al	Mg	Si	Fe	Cu	Cr	Zn	Ti	Mn	others
Min (%)	95.85	0.80	0.40	0	0.15	0.04	0	0	0	0
Max (%)	98.58	1.20	0.80	0.70	0.40	0.35	0.25	0.15	0.15	0.15 total (0.05 ach)

Table 3. The calculation model values.

Constituent	Al	Cr	Cu	Fe	Mg	Mn	Si	Ti	Zn
Min (%)	Balanced	0.05	0	0	4.0	0.4	0	0	0
Max (%)	Balanced	0.25	0.1	0.4	4.9	1.0	0.4	0.15	0.25

– The coil is composed of 3 layers, 20 turns each, and inner radius of 23 mm and outer radius of 29 mm, all coils are made of copper wires with as cross-sectional are of 2 mm × 4 mm and 80 mm height.
– The magnetic field shaper is placed coaxially between the workpiece and the coil with side spacing of 1.25 mm and is of 6 mm thickness. The converter is made of high-conductivity copper material.
– The piece of metal (workpiece) considered in this paper is round Aluminum Alloy 5083 (AA5083) tube that has a height of 130 mm, a 2 mm thickness, with inner radius of 37.5 mm, a 39.5 mm outer radius. **Figure 8** and **Figure 9** show the Model structure used after simulation (coil, field shaper and Tube) and Symmetrical model of 2D state, after air models are established.

When a time-varying pulse current passes through the forming coil, a time-varying magnetic field is generated in the vicinity of the coil that can be expressed by the below equations.

$$\nabla \times \boldsymbol{H} = \boldsymbol{J} \tag{8}$$

$$\nabla \times \boldsymbol{E}_{\varphi} = -\frac{\partial \boldsymbol{B}_z}{\partial t} + \nabla \times \left(\boldsymbol{v}_z \times \boldsymbol{B}_r \right) \tag{9}$$

$$\nabla \cdot \boldsymbol{B} = 0 \tag{10}$$

$$\boldsymbol{J}_{\varphi} = \gamma \boldsymbol{E}_{\varphi} \tag{11}$$

From the above equations we know that $\boldsymbol{B}$ is the magnetic flux density; $\boldsymbol{E}$ is the electric field intensity; $\boldsymbol{v}$ is the pipe fitting speed which is 0 at the initial state, $\boldsymbol{J}$ is the induced eddy current density; γ is the pipe conductivity [26]. The subscripts r, φ, and z represent respectively the radial, hoop and axial components of the vector. The electromagnetic force density $\boldsymbol{F}$ is calculated using the equation (12).

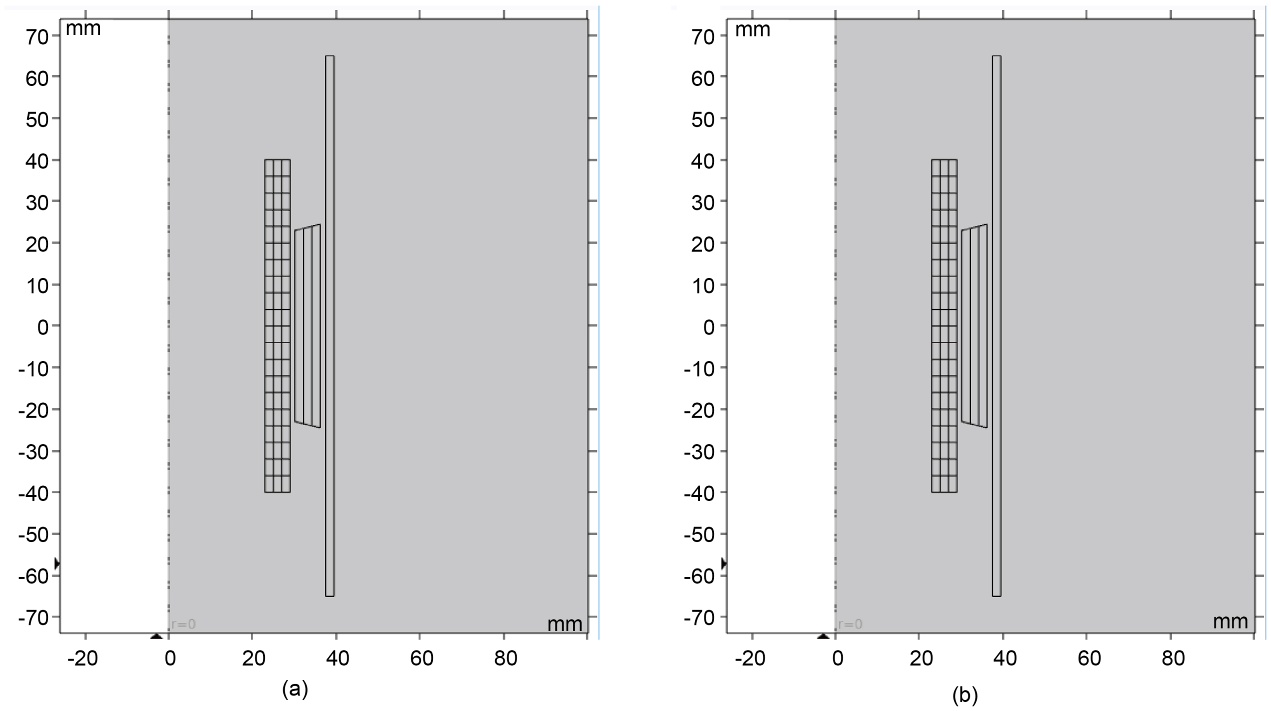

Figure 8. Model structure (coil, field shaper and tube).

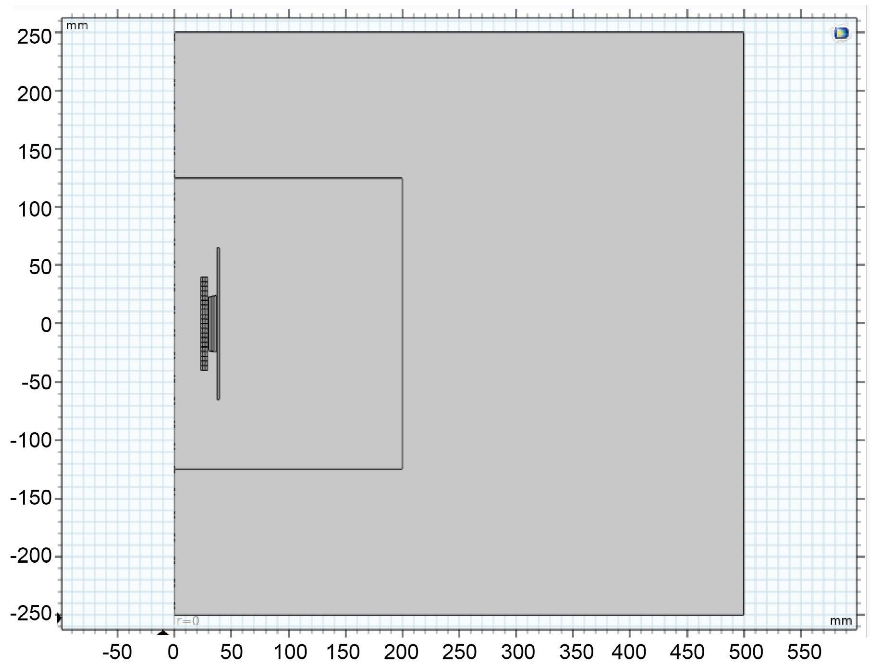

Figure 9. Symmetrical model of 2D state, after air models are established.

$$\boldsymbol{F} = \boldsymbol{J} \times (\nabla \times \boldsymbol{A}) \tag{12}$$

The designed model in this paper has axial symmetry. Therefore, the induced eddy current has only a circumferential direction, and the electromagnetic force density is calculated from:

$$\boldsymbol{F}_z = \boldsymbol{J}_\varphi \times \boldsymbol{B}_r \tag{13}$$

$$\boldsymbol{F}_r = \boldsymbol{J}_\varphi \times \boldsymbol{B}_z \tag{14}$$

$\boldsymbol{F}_z$ and $\boldsymbol{F}_r$ are respectively the axial and radial electromagnetic force densities of the pipe (Tube). $\boldsymbol{J}_\varphi$ is the induced eddy current in the circumferential direction of the tube [27].

Solid Mechanics Module is used to simulate the deformation process of a tube fitting. The relationship between the electromagnetic force and deformation of the pipe fittings is as follows:

$$\boldsymbol{F} = \rho \frac{\partial^2 \boldsymbol{u}}{\partial t^2} - \nabla \cdot \boldsymbol{\sigma} \tag{15}$$

where $\boldsymbol{\sigma}$ is the stress tensor of the pipe, $\boldsymbol{F}$ is the volume density vector of electromagnetic force, ∇ operator for calculating divergence, ρ is the pipe density, $\boldsymbol{u}$ is the displacement vector of the fitting.

One thing that needs to be considered is the change of Aluminum alloy with the strain rate, usually the metal forming speed can vary from 180m/s to 300m/s. For this reason, it is necessary to consider the effect of high speed and high strain rate on the material properties of the tube. The coupling model used in this work is used to simulate the Aluminum alloy AA 5083 tube set up on the following equation.

$$\boldsymbol{\sigma} = \left[1 + \left(\frac{\varepsilon_{p^e}}{P}\right)^m\right] \boldsymbol{\sigma}_{ys} \tag{16}$$

where: $\boldsymbol{\sigma}$, P, m, $\boldsymbol{\sigma}_{ys}$ respectively represent the stress of the tube under high deformation, the viscosity of the tube material, the strain rate hardening of the material and the flow stress under unchanged conditions.

5.3. Material Parameters of the Model

5.3.1. Values from the Equivalent Circuit of EMF

The data values from the equivalent circuit are described below.

Symbol	Description	Value
$\boldsymbol{C_o}$	Capacitance	320 µF
$\boldsymbol{U_o}$	Discharge voltage	6.4 kv
$\boldsymbol{L_o}$	Line inductance	12 µF
$\boldsymbol{R_d}$	The crowbar resistance	0.2 Ω
$\boldsymbol{R_o}$	the line resistance	35 mΩ
$\boldsymbol{S}$	Cross sectional area of the wire	2×4 mm^2

5.3.2. Coil Data Value

(a) Dimensions

Name	Numerical value	Unit
Radial layers number	3	
Number of turns	20	
Inner radius	23	Mm
Outer radius	29	Mm
Wire type (radial × axial)	2 × 4	mm × mm (mm^2)
Height	80	Mm

(b) Properties

Symbol	Description	Value
ρ_{coil}	Pipe Density	8700 Kg/m^3
C_p	Heat capacity	385 J/kg.K
σ_{coil}	Initial yield stress	32.6 MPa
E_{coil}	Young's modulus	70 GPa
V	Poisson's ration	0.33
Σ_{coil}	Electrical conductivity	5,998 × 10^7 S/m
ε_{coil}	Relative permittivity	1
ε_o	Surface emissivity	0.5
K	Thermal conductivity	400 W/m
ρ_o	Reference resistivity	1.662 × 10^8 Ω·m
α	Resistivity temperature coefficient	3.862 × 10^{-3} /K
♣	Reference temperature	293.15 K

The properties of the above table (b) are the same for the electromagnetic field shaper.

5.3.3. Field Shaper Data Value

Name	Numerical value	Unit
Space between coil & Field shaper	1.25	Mm
Thickness	6	Mm

5.3.4. Workpieces (AA 5083) Properties Data Value

Symbol	Description	Value
r_{in}	Tube inner radius	37.5 mm
r_{out}	Tube outer radius	39.5 mm
H_t	Tube height	130 mm
ρ	Pipe Density	2700 Kg/m^3

Continued

σ_{yso}	Initial yield stress	32.6 MPa
E	Young's modulus	70 GPa
V	Poisson's ration	0.33
σ	Electrical conductivity	3,03e7 S/m
ε	Relative permittivity	1
μ_r	Relative permeability	1

6. Simulation Findings

After analyzing the full process using the simulation result, we found that when the system parameters remain unchanged, the distribution of the radial electromagnetic force will be the main parameter affecting the uniformity of the axial deformation of the tube, observing this simulation result we have seen that the induced eddy current and the strength of the magnetic field together determine the electromagnetic force experienced by the pipe. When the system parameters remain unchanged, the distribution of the radial electromagnetic force will be the main parameter affecting the uniformity of the axial deformation of the pipe. The figures below are the simulation results of the tube during the deformation process with the magnetic flux density, the equivalent plastic train. **Figure 10** shows the 2D simulation of Tube deformation, **Figure 11** shows 2D simulation of magnetic flux density, **Figure 12** shows the 2D Equivalent Plastic strain simulation, **Figure 13** shows the simulation result of the Global equations during the deformation, **Figure 14** shows the 3D simulation of Tube deformation results, **Figure 15** shows the 3D magnetic flux density (Area influenced by the Magnetic field) and **Figure 16** shows the 3D volume density (Area influenced by the deformation), respectively.

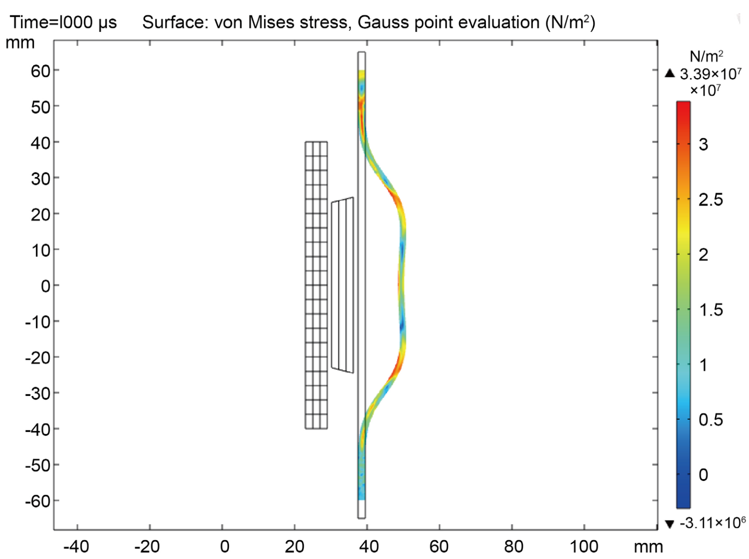

Figure 10. 2D Tube deformation.

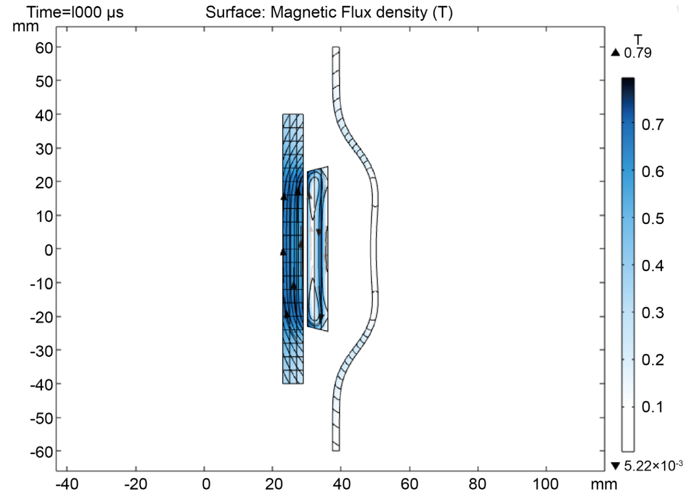

Figure 11. 2D magnetic flux density.

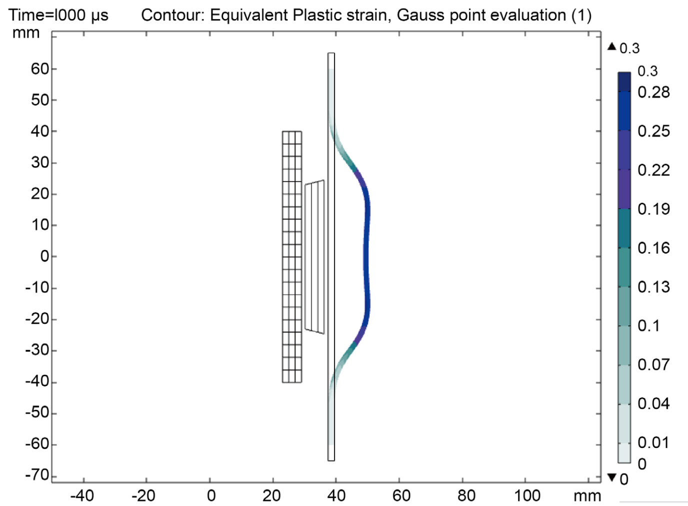

Figure 12. 2D Equivalent Plastic strain.

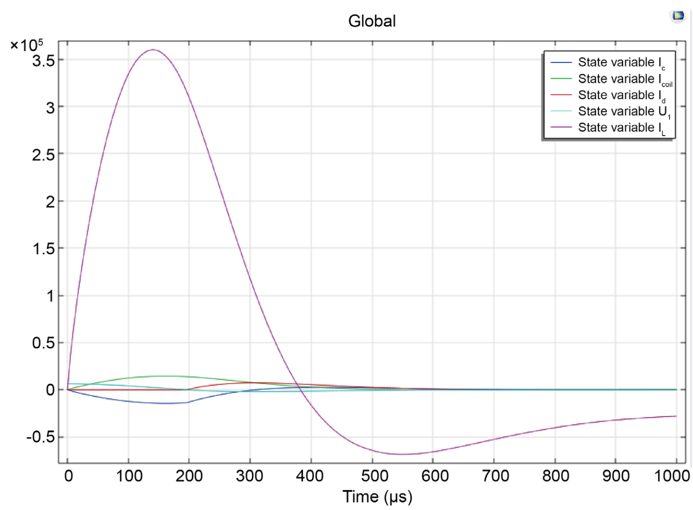

Figure 13. Global equations.

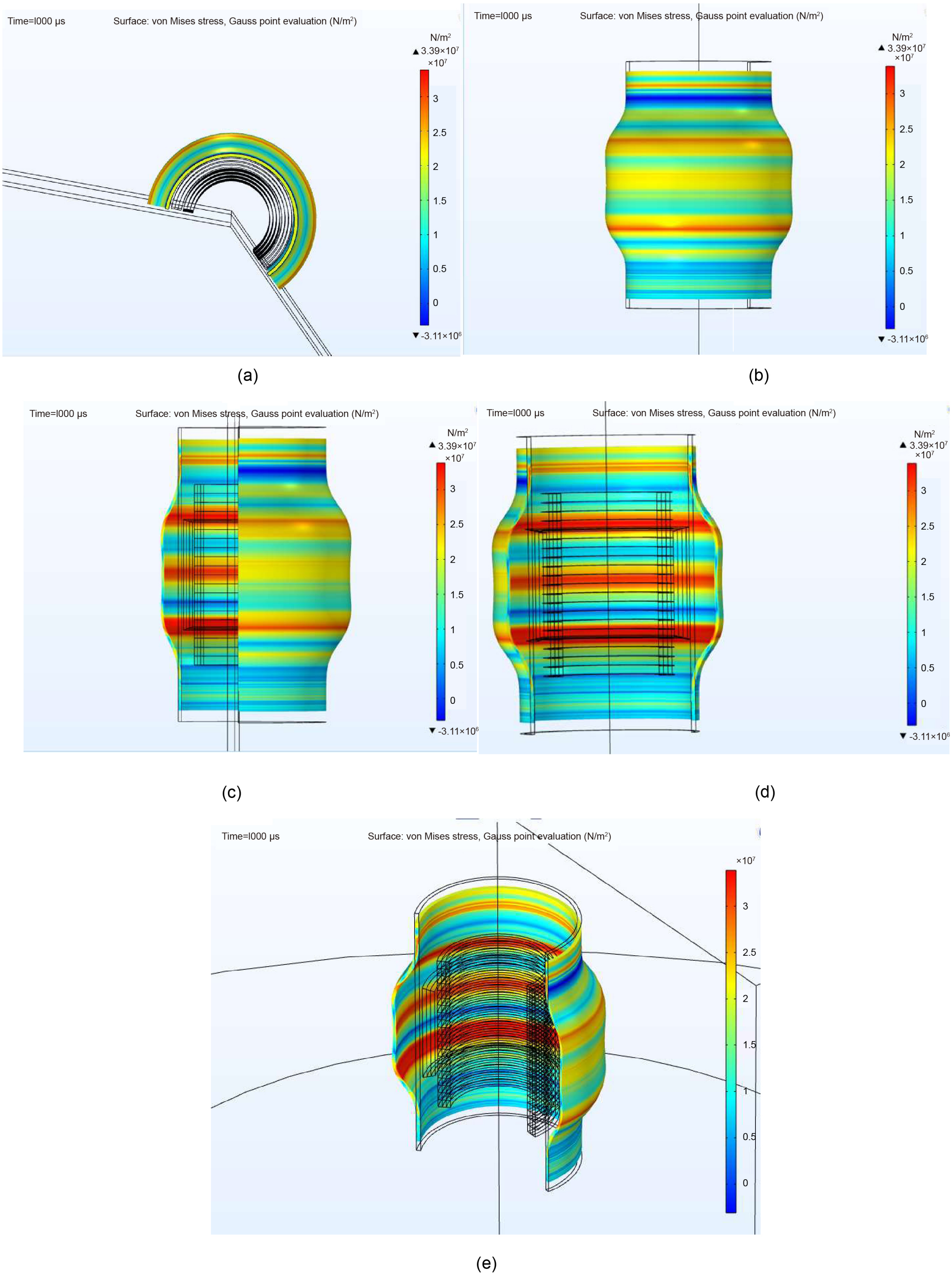

Figure 14. 3D Tube deformation results.

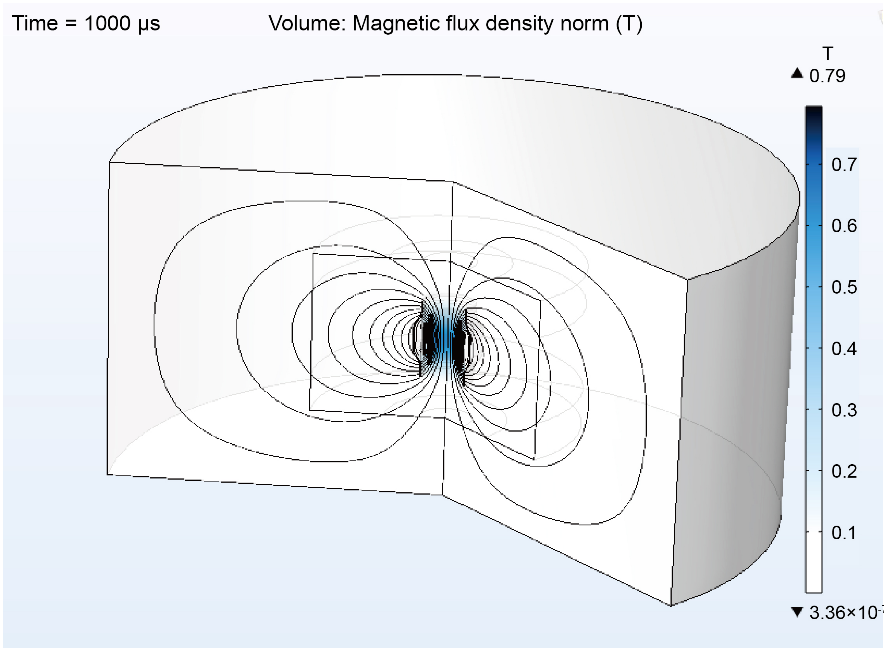

Figure 15. 3D magnetic flux density (area influenced by the magnetic field).

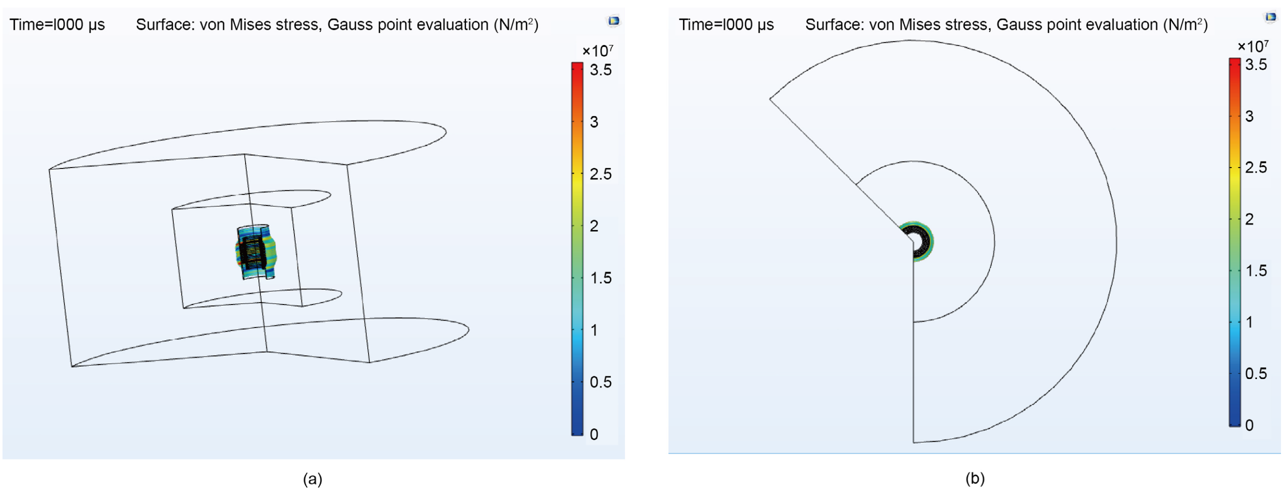

Figure 16. 3D volume density (area influenced by the deformation).

7. Discussion

The most affecting element in this EMF process is the induced eddy current and the strength of the magnetic field (the magnetic flux) and all together they determine the electromagnetic force experienced by the pipe. During this interaction, the transient current flowing through the actuating coil generates a time varying magnetic field. While the EMF forming process time start from 0 µs to 1000 µs and the parameters and position of the coil remain unchanged, we have noticed that the structural change of the tube in terms of its height, the initially the tube's height was 130 mm; once the EMF process has started, the magnetic field collected by the field shaper will be evenly redistributed along the workpiece and this will cause its deformation, in addition a loss in height equivalent to 5 mm at the top and bottom of the workpiece due to the expansion in the middle part of the tube, hence reducing the height of the latter one to 120 mm meanwhile the general length of the tube it is stretched up thanks to the Electromagnetic expansion, the inner radius increase from 37.5 mm to 53 mm.

Furthermore, in order to better illustrate in discussing the situation of the tube deformation during the expansion process, the forming conditions of the tube at different times points when using the coil and magnetic field shaper proposed in this paper are obtained as shown in **Figure 17**. It can be seen that at when t = 250 μs, when the cylindrical coil is loaded, the middle part of the tube starts to deform, and the deformation area of the driving coil based on the magnetic field shaper is larger than traditional bulging process. At t = 1000 μs, the tube reaches it is maximum deformation, and when the cylindrical coil is loaded, and the proposed methods (insertion of a magnetic the field shaper) is employed, the tube is uniformly deformed and the flow of the tube material in the axial direction can be realized.

A 2D model temporal change of the tube through EMF is shown in **Figure 17**.

Figure 17 shows the 2D Temporal deformation process and **Figure 18** shows the 3D simulation model temporal change of the tube through EMF, respectively.

In order to better illustrate that the electromagnetic bulging of tube based on the proposed method can improve the forming uniformity, a 3D graph of the distribution of the eddy current induced on the inner wall of the magnetic field shaper over time is obtained as shown in **Figure 19**. When a traditional coil is used to load the pipe, the driving coil is cylindrically wound and the same driving current is passed. Due to the uniform current distribution, the induced current in the axial direction of the pipe is also uniformly distributed and the pipe has a relatively flat top and the deformation area of the pipe becomes wider. Obviously, the end effect of the electromagnetic bulging of the traditional helical coil tube is weakened to a certain extent and the axial flux density and the corresponding radial electromagnetic force distributions are obtained as shown in **Figure 20**. Furthermore, in order to better reflect the deformation state of the pipe fitting in this discussion, during the expansion process, the forming conditions of the pipe fitting at different times when using the conventional coil and magnetic field shaper proposed in this paper are obtained as shown in **Figure 21**. It can be seen that at t = 100 μs, when the conventional cylindrical coil is loaded, the middle part of the tube begins to deform, and the deformation area of the driving coil based on the magnetic field shaper is larger. At t = 600 μs, the tube reaches a maximum deformation, and when the traditional cylindrical coil is loaded, the axial deformation of the tube is uneven and exhibits a convex distribution. **Figure 19** shows the distribution of induced eddy current with time and axial position, **Figure 20** shows the axial flux density and the corresponding radial electromagnetic force distributions, **Figure 21** shows the 2D Temporal deformation process of the traditional Electromagnetic forming at different times and **Figure 22** shows the Temporal deformation process of the EMF with the magnetic field shaper, respectively.

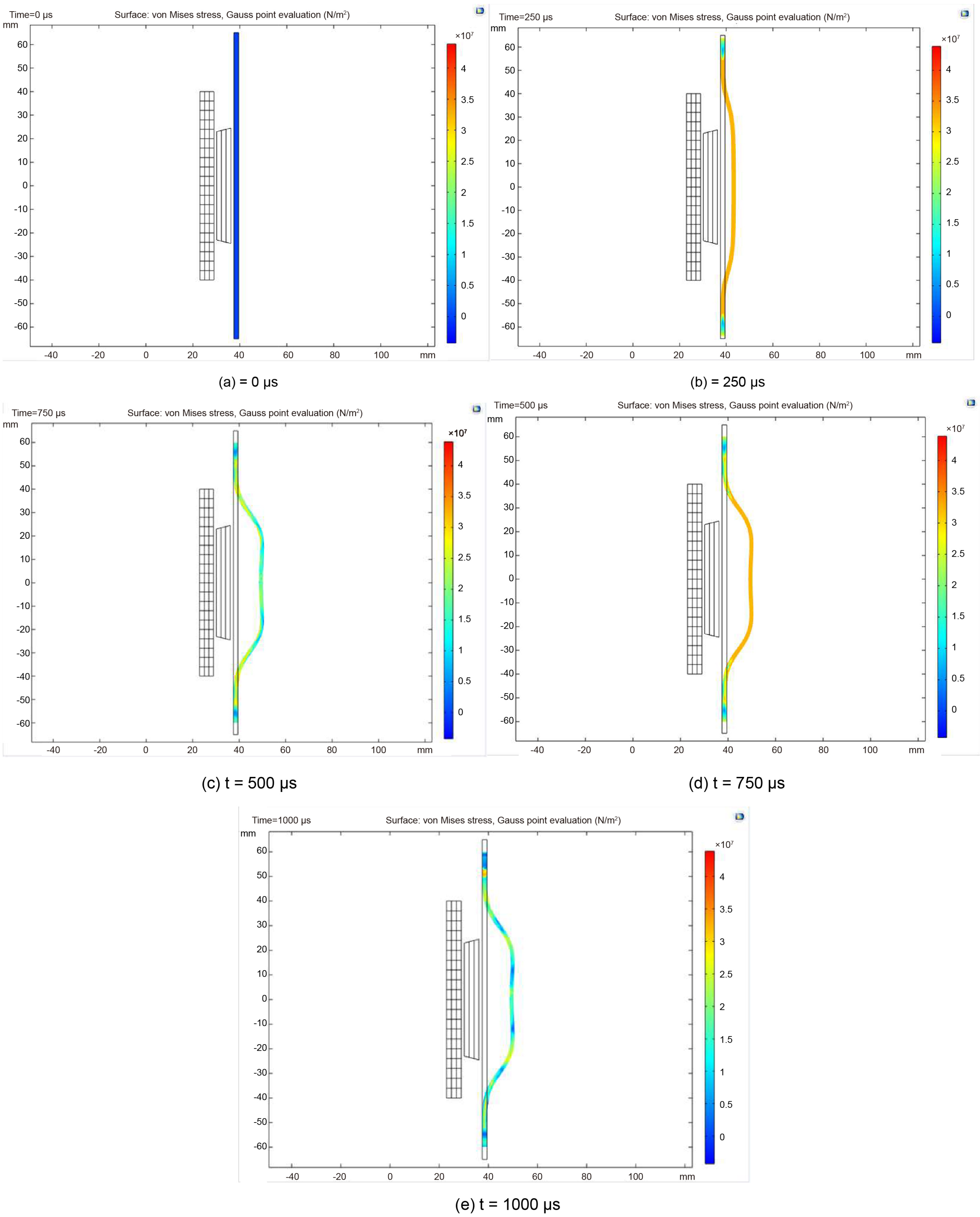

Figure 17. 2D Temporal deformation process.

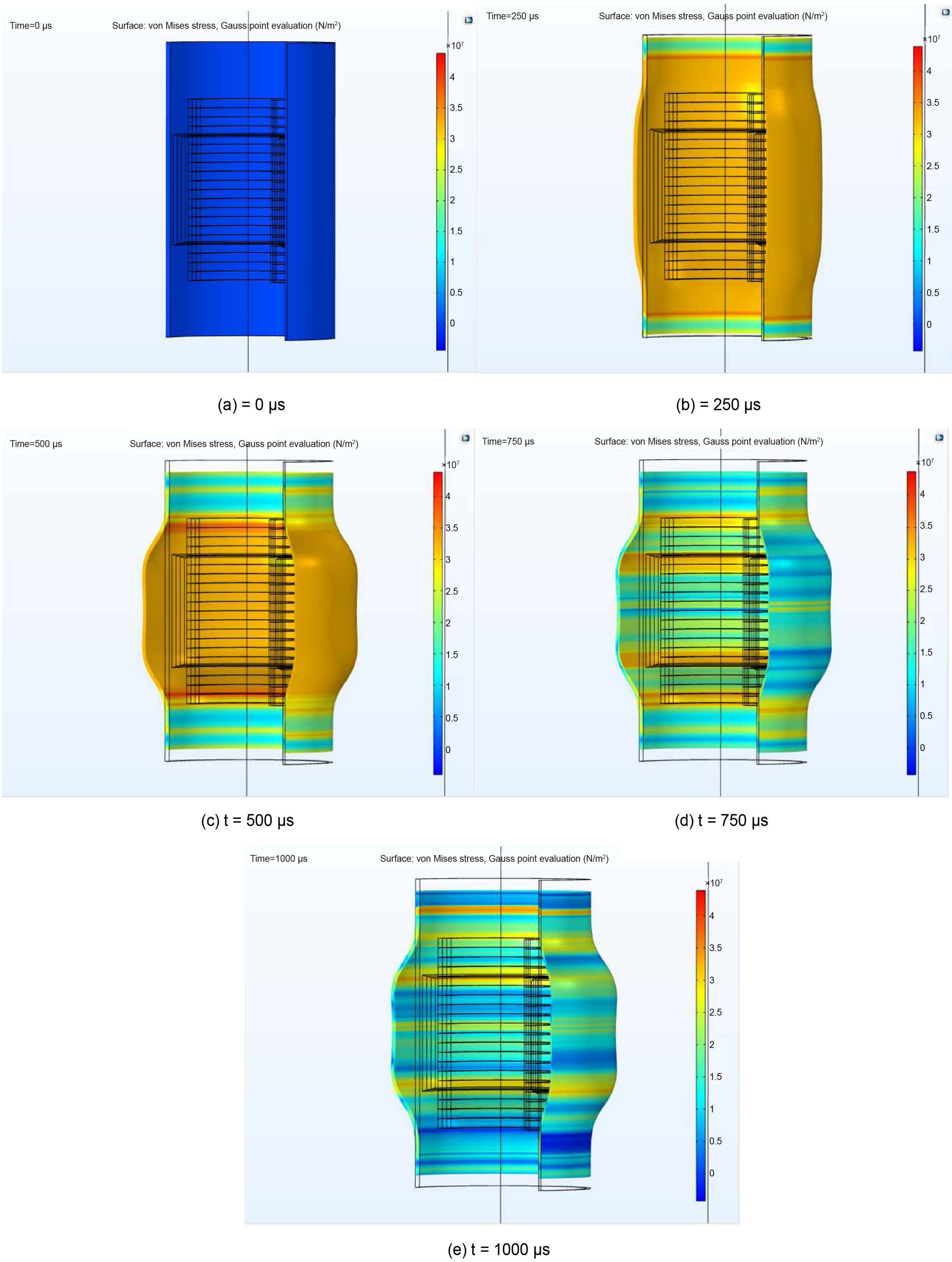

Figure 18. 3D Temporal deformation process.

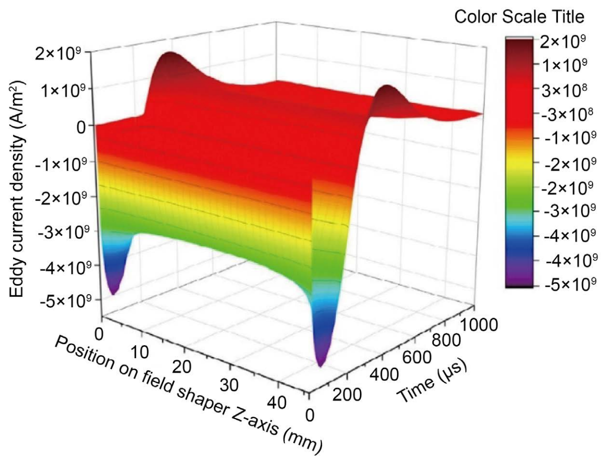

Figure 19. Distribution of induced eddy current with time and axial position.

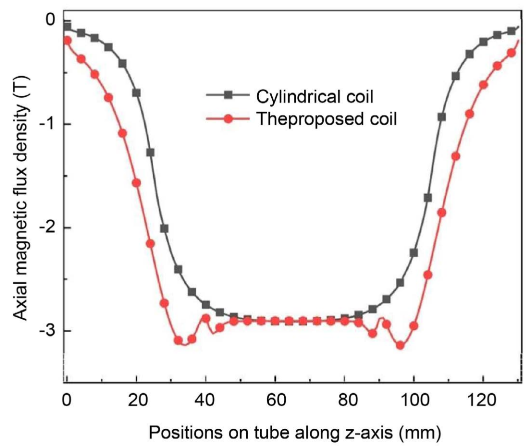

Figure 20. The axial flux density and the corresponding radial electromagnetic force distributions.

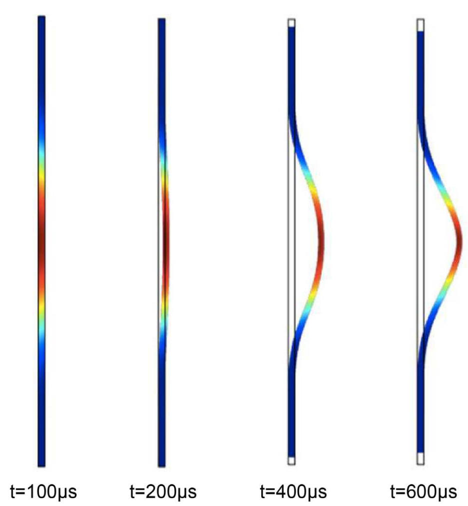

Figure 21. 2D Temporal deformation process of the traditional electromagnetic forming at different times.

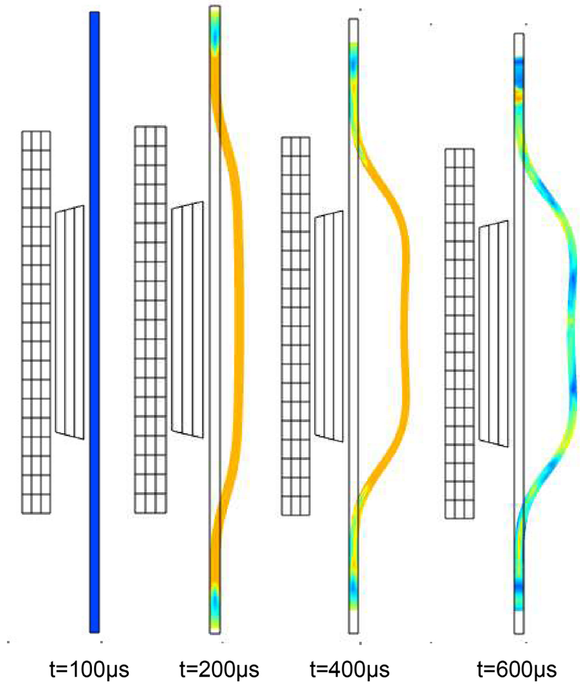

Figure 22. 2D Temporal deformation process of the EMF with the magnetic field shaper.

8. Conclusions

The practicability of the suggested technique to control the electromagnetic force distribution profile is verified through the results which reveal that when the proposed method is employed, the radial-electromagnetic force becomes of convex-distribution which can remarkably increase the end deformation of the workpiece, overcome the end effect of the conventional forming process of pipe fitting, and uniformize the axial deformation of the tube more.

From the simulation we have seen that when the system discharge parameters remain the same, there is a suitable magnetic field shaper structure parameter that optimizes the electromagnetic forming. By placing a magnetic field shaper between the driving coil and the workpiece, the distribution of the induced eddy current in the tube can be considerably controlled and well regulated, thereby realizing the loading of different electromagnetic force distributions which can effectively overcome the end effect in the traditional electromagnetic forming process and strengthen the radial electromagnetic force at both ends of the tube fitting, while weakening it at the middle of the tube, hence uniformizing the radial deformation of the tube.

9. The Future Work

This feature facilitates the new EMF method to realize the processing requirements for different metal pieces. While the feasibility of the proposed Electromagnetic Forming technique is proven in this paper through detailed finite element analysis, further validation through experimental measurements including the discussion regarding the safety measures necessary when dealing with high Lorentz forces and the potential high-speed metal deformation process risks, the durability issues of the field shaper under high electromagnetic forces and the raising concerns about the long-term feasibility and maintenance costs are to be presented in our future work.

Conflicts of Interest

The authors declare no conflicts of interest regarding the publication of this paper.

References

[1] Ouyang, S., Li, X., Li, C., Du, L., Peng, T., Han, X., *et al.* (2020) Investigation of the Electromagnetic Attractive Forming Utilizing a Dual-Coil System for Tube Bulging. *Journal of Manufacturing Processes*, **49**, 102-115. https://doi.org/10.1016/j.jmapro.2019.11.006

[2] Cao, Q., Du, L., Li, Z., Lai, Z., Li, Z., Chen, M., *et al.* (2019) Investigation of the Lorentz-Force-Driven Sheet Metal Stamping Process for Cylindrical Cup Forming. *Journal of Materials Processing Technology*, **271**, 532-541. https://doi.org/10.1016/j.jmatprotec.2019.03.002

[3] Qiu, L., Zhang, W., Abu-Siada, A., Xiong, Q., Wang, C., Xiao, Y., *et al.* (2020) Electromagnetic Force Distribution and Wall Thickness Reduction of Three-Coil Electromagnetic Tube Bulging with Axial Compression. *IEEE Access*, **8**, 21665-21675. https://doi.org/10.1109/access.2020.2969678

[4] Qiu, L., Wang, B., Abu-Siada, A., Xiong, Q., Zhang, W., Ge, W., *et al.* (2020) Research on Forming Efficiency in Double-Sheet Electromagnetic Forming Process. *IEEE Access*, **8**, 19248-19255. https://doi.org/10.1109/access.2020.2968049

[5] Qiu, L., Yi, N., Abu-Siada, A., Tian, J., Fan, Y., Deng, K., *et al.* (2020) Electromagnetic Force Distribution and Forming Performance in Electromagnetic Forming with Discretely Driven Rings. *IEEE Access*, **8**, 16166-16173. https://doi.org/10.1109/access.2020.2967096

[6] Qiu, L., Wang, C., Abu-Siada, A., Xiong, Q., Zhang, W., Wang, B., *et al.* (2020) Coil Temperature Rise and Workpiece Forming Efficiency of Electromagnetic Forming Based on Half-Wave Current Method. *IEEE Access*, **8**, 9371-9379. https://doi.org/10.1109/access.2020.2965254

[7] Huang, L., Zhang, J., Zou, J., Zhou, Y. and Qiu, L. (2019) Effect of Equivalent Radius of Drive Coil on Forming Depth in Electromagnetic Sheet Free Bulging. *International Journal of Applied Electromagnetics and Mechanics*, **61**, 377-389. https://doi.org/10.3233/jae-190009

[8] Cao, Q., Li, Z., Lai, Z., Li, Z., Han, X. and Li, L. (2018) Analysis of the Effect of an Electrically Conductive Die on Electromagnetic Sheet Metal Forming Process Using the Finite Element-Circuit Coupled Method. *The International Journal of Advanced Manufacturing Technology*, **101**, 549-563. https://doi.org/10.1007/s00170-018-2798-8

[9] Zhang, X., Cao, Q., Han, X., Chen, Q., Lai, Z., Xiong, Q., *et al.* (2016) Application of Triple-Coil System for Improving Deformation Depth of Tube in Electromagnetic Forming. *IEEE Transactions on Applied Superconductivity*, **26**, Article ID: 3701204. https://doi.org/10.1109/tasc.2016.2542482

[10] Li, X.X., Cao, Q.L., Lai, Z.-P., *et al.* (2020) Bulging Behavior of Metallic Tubes during the Electromagnetic Forming Process in the Presence of a Background Magnetic Field. *Journal of Materials Processing Technology*, **276**, Article ID: 116411.

[11] Cao, Q.L., Li, X., Li, Z.H., *et al.* (2021) Coil-less Electromagnetic Forming Process with Uniform-Pressure Characteristics for Shaping Sheet Metals. *Journal of Manufacturing Processes*, **70**, 140-151.

[12] Niayesh, K. and Karimi, A. (2006) Application of Field-Shapers to Localize Applied Forces during Impulse Electromagnetic Forming Process. 51*st Internationales Wissenschaftliches Kolloquium*, Ilmenau, 11-15 September 2006, 140-146.

[13] Shanthala, K. and Sreenivasa, T.N. (2015) Stress Analysis of Field Shaper in ElectroMagnetic Welding. *International Journal of Scientific Research*, **4**, 3-5.

[14] Yu, H.P., Zhao, C. and Li, Z. (2005) Effect of Field Shaper on Magnetic Pressure in Electromagnetic Forming. *Journal of Materials Processing Technology*, **168**, 245-249.

[15] Li, J.J., Li, L., Wan, M., Yu, H.P. and Liu, L. (2018) Innovation Application of Electromagnetic Forming and Its Fundamentals Problems. *Procedia Manufacturing*, **15**, 14-30.

[16] Ma, H., Huang, L., Li, J., Duan, X. and Ma, F. (2018) Effects of Process Parameters on Electromagnetic Sheet Free Forming of Aluminium Alloy. *The International Journal of Advanced Manufacturing Technology*, **96**, 359-369. https://doi.org/10.1007/s00170-018-1589-6

[17] Bach, F., Bormann, D. and Walden, L. (2008) Influence of Forming Rate on the Microstructure and Properties of Materials Subjected to Electromagnetic Forming: A Synopsis. Universitätsbibliothek Dortmund.

[18] Feng, F., Huang, S., Meng, Z., Hu, J., Lei, Y., Zhou, M., *et al.* (2014) Experimental Study on Tensile Property of AZ31B Magnesium Alloy at Different High Strain Rates and Temperatures. *Materials & Design*, **57**, 10-20. https://doi.org/10.1016/j.matdes.2013.12.031

[19] Ma, H., Huang, L., Wu, M. and Li, J. (2014) Dynamic Ductility and Fragmentation for Aluminum Alloy Using Electromagnetic Ring Expansion. *Procedia Engineering*, **81**, 787-792. https://doi.org/10.1016/j.proeng.2014.10.077

[20] Qiu, L., Yu, Y., Wang, Z.W., *et al.* (2018) Analysis of Electromagnetic Force and Deformation Behavior in Electromagnetic Forming with Different Coil Systems. *International Journal of Applied Electromagnetics and Mechanics*, **57**, 337-345.

[21] Gayakwada, D., Dargar, M.K., Sharma, P.K., *et al.* (2014) A Review on Electromagnetic Forming Process. *Procedia Materials Science*, **6**, 520-527.

[22] Shim, J.-Y. and Kang, B.-Y. (2015) Development of Aluminum Small Digital Electronics Cases Using Magnetic Pulse Forming Process.

[23] Backus, D.L. (2013) The Effect of a Field Shaper on Electromagnetic Forming of Aluminum Tubes.

[24] Xiong, Q., Gao, D., Li, Z., Yang, M., Zhu, X. and Zhao, X. (2021) Electromagnetic Attraction Bulging of Small Aluminum Alloy Tube Based on a Field Shaper. *The International Journal of Advanced Manufacturing Technology*, **117**, 511-521. https://doi.org/10.1007/s00170-021-07732-w

[25] Gawade, S., Date, P.P. and Sharma, S.B. (2011) On the Simulation of Electromagnetic Forming Process of Tube Using Multiphysics Software.

[26] Kumar, R. (2020) Studies on the Effect of Surface Profiles and Field Shaper Geometries on Electromagnetic Crimping of Tubes on Rods.

[27] Qiu, L., Wang, C.L., Abu-Siada, A., *et al*. (2020) Numerical Analysis of Tube Expansion by Electromagnetic Forming Using Magnetic Field Shaper. *IEEE Access*, **8**, 196253-196263.